

LA-UR-16-24836

Approved for public release; distribution is unlimited.

Report on in-situ studies of flash sintering of uranium dioxide Title:

Author(s):

Raftery, Alicia Marie Knudson, Frances Lynn

Intended for: Report

2017-01-24 (rev.1) Issued:



Report on in-situ studies of flash sintering of uranium dioxide

Fuel Cycle Research & Development

Prepared for U.S. Department of Energy FCRD program Alicia M. Raftery Los Alamos National Laboratory 7/01/16



DISCLAIMER

This information was prepared as an account of work sponsored by an agency of the U.S. Government. Neither the U.S. Government nor any agency thereof, nor any of their employees, makes any warranty, expressed or implied, or assumes any legal liability or responsibility for the accuracy, completeness, or usefulness, of any information, apparatus, product, or process disclosed, or represents that its use would not infringe privately owned rights. References herein to any specific commercial product, process, or service by trade name, trade mark, manufacturer, or otherwise, does not necessarily constitute or imply its endorsement, recommendation, or favoring by the U.S. Government or any agency thereof. The views and opinions of authors expressed herein do not necessarily state or reflect those of the U.S. Government or any agency thereof.

SUMMARY

Flash sintering is a novel type of field assisted sintering that uses an electric field and current to provide densification of materials on very short time scales. The potential for field assisted sintering techniques to be used in producing nuclear fuel is gaining recognition due to the potential economic benefits and improvements in material properties. The flash sintering behavior has so far been linked to applied and material parameters, but the underlying mechanisms active during flash sintering have yet to be identified.

This report summarizes the efforts to investigate flash sintering of uranium dioxide using dilatometer studies at Los Alamos National Laboratory and two separate sets of in-situ studies at Brookhaven National Laboratory's NSLS-II XPD-1 beamline. The purpose of the dilatometer studies was to understand individual parameter (applied and material) effects on the flash behavior and the purpose of the in-situ studies was to better understand the mechanisms active during flash sintering.

As far as applied parameters, it was found that stoichiometry, or oxygen-to-metal ratio, has a significant effect on the flash behavior (time to flash and speed of flash). Composite systems were found to have degraded sintering behavior relative to pure UO_2 . The critical field studies are complete for $UO_{2.00}$ and will be analyzed against an existing model for comparison.

The in-situ studies showed that the strength of the field and current are directly related to the sample temperature, with temperature-driven phase changes occurring at high values. The existence of an 'incubation time' has been questioned, due to a continuous change in lattice parameter values from the moment that the field is applied. Some results from the in-situ experiments, which should provide evidence regarding ion migration, are still being analyzed.

Some preliminary conclusions can be made from these results with regard to using field assisted sintering to fabricate nuclear fuel. First, the pure UO₂-based system shows promising behavior with flash sintering, but composite systems are likely to show better sintering behavior with spark plasma sintering. Efforts to develop these methods should therefore be tailored towards the likelihood of success. Additionally, modeling is a rapidly developing aspect of current flash sintering research and should be used in parallel with experiments. Ultimately, ongoing flash sintering studies on various materials, like those summarized in this report, are rapidly contributing to the feasibility of controlling this method for use in the future

Table of Contents

1. INTRODUCTION	1
1.1 Conventional Sintering	1
1.2 Field Assisted Sintering	2
1.2.1 Spark Plasma Sintering	2
	3
1.3 FAS Application to ATF	4
2. Experimental	5
	5
	6
	6
2.2.2 In-situ	6
2 Initial Studios	
	½ System
	2 System
	10
	11
	11
	11
1	
5. In-situ Studies at Brookhaven NSLS	-II14
	14
	gth and Current Density14
	14
•	
	on Time and Scanning19
*	
	20
5.3.3 Scanning Experiments	22
6. Key Observations to Date	23
7. Recommendations/Path Forward	24
O Deferences	25

FIGURES

Figure 1. Conventional sintering curve showing the temperature profile (blue line) and densification profile (black line) of UO_2 at $1000^{\circ}C$. Densification is represented in percent theoretical density (%TE and change in length (dL/L_o))) 1
Figure 2. Schematic of the SPS method, with all components labeled [4]	2
Figure 3. Figure 3. SPS parameter profile for UO ₂ displaying temperature, z-axis pressure, and z-axis displacement during sintering [5]	2
Figure 4. Schematic of flash sintering setup with main components labeled [7]	3
Figure 5. Current and voltage parameter profile during FS of UO ₂ (100 V/cm, 125 mA/mm ²)	3
Figure 6. Microstructure of a UO ₂ -SiC composite sintered using SPS [9]	∠
Figure 7. Dimensions of rectangular geometry samples (7mm x 1 mm x 2 mm) used for the in-situ studies	5
Figure 8. Pellet sample (D = 4.75mm) loaded in dilatometer with leads in contact with ends	<i>6</i>
Figure 9. (a) Overview of in-situ experimental setup and (b) close-up of sample loaded	е
Figure 10. Current runaway for three applied field strengths on a UO _{2.16} rectangular sample, showing that the increase in field strength results in an enhancement in the flash behavior	7
Figure 11. Current runaway for three starting material densities of UO _{2.00} rectangular samples, showing that lower density enhances the flash behavior	8
Figure 12. Power transient behavior for flashing of pure UO ₂ and composite systems	8
Figure 13. Comparison of YSZ results with flash sintering curves by Francis [15]	9
Figure 14. Field strength vs. step time for varying material (system) resistance	10
Figure 15. Step time results for alternating anode and cathode leads on a UO _{2.16} rectangular sample	11
Figure 16. Influence of the voltage ramp rate on (a) field strength at flash and (b) step time of UO _{2.16} pellet geometry sample	12
Figure 17. Critical field results for UO _{2.00} with 1 V/s voltage ramp at isothermal temperature	12
Figure 18. Flow-chart describing thermal runaway process	13
Figure 19. Example of bifurcation theory used to determine critical field points [20]	13
Figure 20. View of XPD-I beamline with experimental equipment	14
Figure 21. In-situ (a) sample geometry and (b) sample clamped and loaded into alumina holder	15

Figure 22. Voltage/current parameter profile during low voltage/low current flash of UO _{2.16}	15
Figure 23. Lattice parameter changes for UO_2 (red) and U_4O_9 (blue) during low voltage/low current flash of $UO_{2.16}$	16
Figure 24. Voltage/current parameter profile during high field/high current flash	17
Figure 25. Lattice parameter changes for UO_2 (red) and U_4O_9 (blue) during low field/low current flash of $UO_{2.16}$	17
Figure 26. Oxygen-Uranium phase diagram, highlighting how conversion would occur for UO _{2.16} [21]	18
Figure 27. Parameter profile with changes in peaks sequentially labeled for high voltage/high current flash of UO _{2.16}	19
Figure 28. Diagram of spring-loaded alumina sample holder	19
Figure 29. Example of flash parameter profile with incubation time	20
Figure 30. Lattice parameter evolution and current flow during flash of UO _{2.00}	21
Figure 31. Lattice parameter evolution and current flow during flash of UO _{2.23}	22
Figure 32. Evidence of a phase transition occurring in U ₄ O ₉ at 75°C [21]	22
TABLES	
Table 1. List of key parameters screened in initial experiments	7
Table 2. Phase content and lattice parameter values for before and after low voltage/low current flash of $UO_{2.16}$	16
Table 3. Phase content and lattice parameter values for before and after high voltage/low current flash of UO _{2.16}	18

7/01/2016 vii

ACRONYMS

AC Alternating Current
AFC Advanced Fuel Cycle
ATF Accident Tolerant Fuel
BNL Brookhaven National Lab

CTE Coefficient of Thermal Expansion

DC Direct Current
DIL Dilatometer

DOE Department of Energy
FAS Field Assisted Sintering

FS Flash Sintering

FCRD Fuel Cycle Research and Development
I-NERI International Nuclear Energy Initiative

LANL Los Alamos National Lab

NSLS National Synchrotron Light Source NTC Negative temperature coefficient

O/M Oxygen-to-Metal ratio
SPS Spark Plasma Sintering
TD Theoretical Density
XRD X-Ray Diffraction

YSZ Yttria Stabilized Zirconia

FCRD ADVANCED FUELS CAMPAIGN

1. INTRODUCTION

Uranium dioxide fuel pellets are used to power the majority of commercial nuclear reactors, with more than 50 years of experience acting as the foundation for its use as a nuclear fuel. Uranium dioxide has a number of properties that are favorable for nuclear fuel, including a high melting temperature (~2850°C), good corrosion resistance, and relatively low swelling under irradiation [1]. However, the recent accident at Fukushima Daiichi in 2011 has highlighted some shortcomings in this well-established fuel, specifically the low thermal conductivity. The fuel research community has therefore decided to address these shortcomings through the pursuit of advanced fuel cycle (AFC) materials in the form of accident tolerant fuel (ATF).

Improvements in the fuel properties can be made by either altering the current fuel or by changing the fuel type entirely. The first option is being pursued in the form of UO_2 composite fuel research and the second through assessment of alternative fuel types (nitrides, silicides). In order to minimize the economic impact, the transition to a new fuel type would preferably use the same fuel geometry and existing infrastructure for the fabrication process. However, relatively new sintering methods now offer the possibility to lower the economic impact of fabrication and to produce high-density composite materials. For this reason, these sintering methods are being investigated for potential use in fabricating ATF.

1.1 Conventional Sintering

Conventional sintering is a process where a ceramic powder compact is placed into a furnace and heated to a temperature close to its melting point in order to cause densification. Through this process, the starting powder is transformed into a dense solid. This is the typical sintering route taken during nuclear fuel fabrication, with furnaces sintering large batches of fuel pellets. Sintering temperatures are as high as 1700°C -1800°C with sintering times of 4-5 hours in order to obtain the necessary high density of 95% theoretical density (TD). There have been numerous efforts in an attempt to lower the sintering temperature to improve efficiency [2]. However, any improvements made in sintering temperature still require long sintering times (hours) since the process is diffusion controlled. Figure 1 shows a densification curve for UO₂ sintered in gettered argon at 1000°C. After 3.5 hours at this high temperature, only 87% TD is reached.

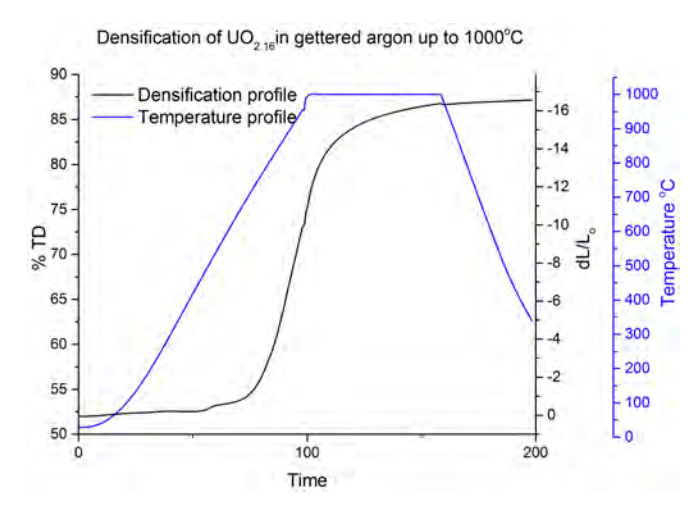


Figure 1. Conventional sintering curve showing the temperature profile (blue line) and densification profile (black line) of UO_2 at $1000^{\circ}C$. Densification is represented in percent theoretical density (%TD) and change in length (dL/L_0).

1.2 Field Assisted Sintering

Field assisted sintering (FAS) describes a group of novel sintering methods that use an electric field and/or current in order to provide powder densification. These methods have proven to provide a higher level of densification in much shorter time periods compared to conventional sintering. The focus in this report will be on the specific methods currently under investigation for nuclear fuel fabrication: spark plasma sintering (SPS) and flash sintering (FS).

1.2.1 Spark Plasma Sintering

Spark plasma sintering is a FAS method that uses the combination of temperature, pressure, and electric current to sinter powder compacts. For this method, powder is loaded into a graphite die and heated by a pulsed direct current (DC) while simultaneously applying a uniaxial pressure. A schematic of this technique is shown in Figure 2. Typically, the applied field is low (~volts) and the permitted current flow through the die is high (~thousands of amps). Advantages of this sintering method include lower sintering temperatures, better mechanical properties, and shorter holding times (minutes) [3]. The typical sintering parameter profile for SPS is shown in Figure 3, highlighting how the applied pressure aids in densification.

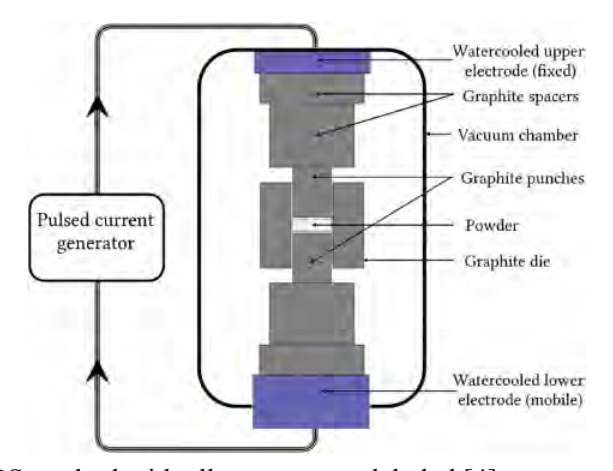


Figure 2. Schematic of the SPS method with all components labeled [4].

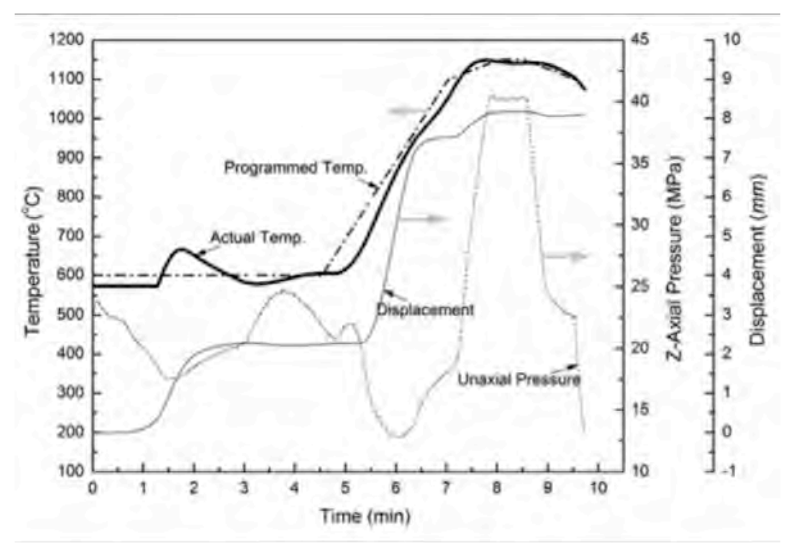


Figure 3. SPS parameter profile for UO₂ displaying temperature, z-axis pressure, and z-axis displacement during sintering [5].

1.2.2 Flash Sintering

Flash sintering is similar to SPS in that it uses an electrical field (and current) to induce sintering. However, the applied field is high (hundreds of volts) and the current flow through the sample is low (amps). The typical flash sintering setup includes a sample placed in a furnace, with two leads in contact and attached to a power supply, shown in Figure 4. The "flash" is characterized by a current runaway, in which the current exponentially increases until reaching a pre-defined current limit. This runaway behavior is illustrated below in Figure 5, which shows the current/voltage behavior during flash sintering of UO_2 . The bulk of sintering can occur on the order of seconds under the application of a high field and high temperature [6].

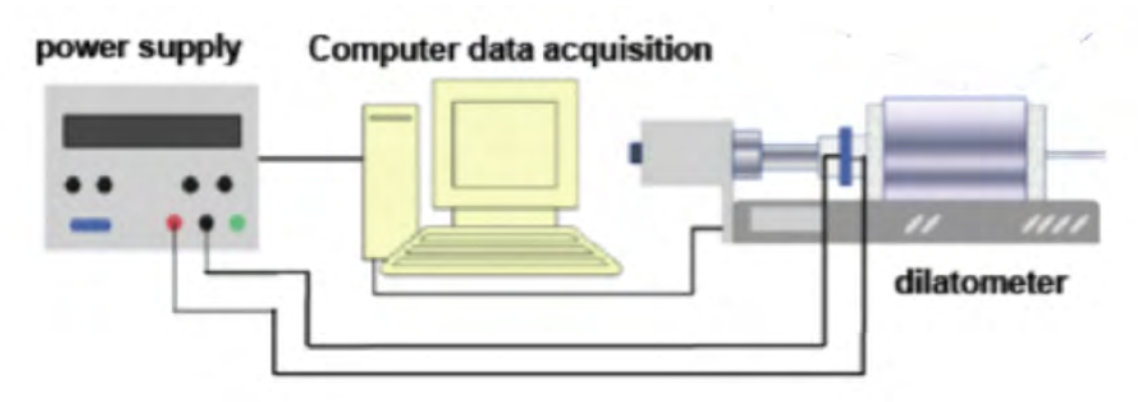


Figure 4. Schematic of flash sintering setup with main components labeled [7].

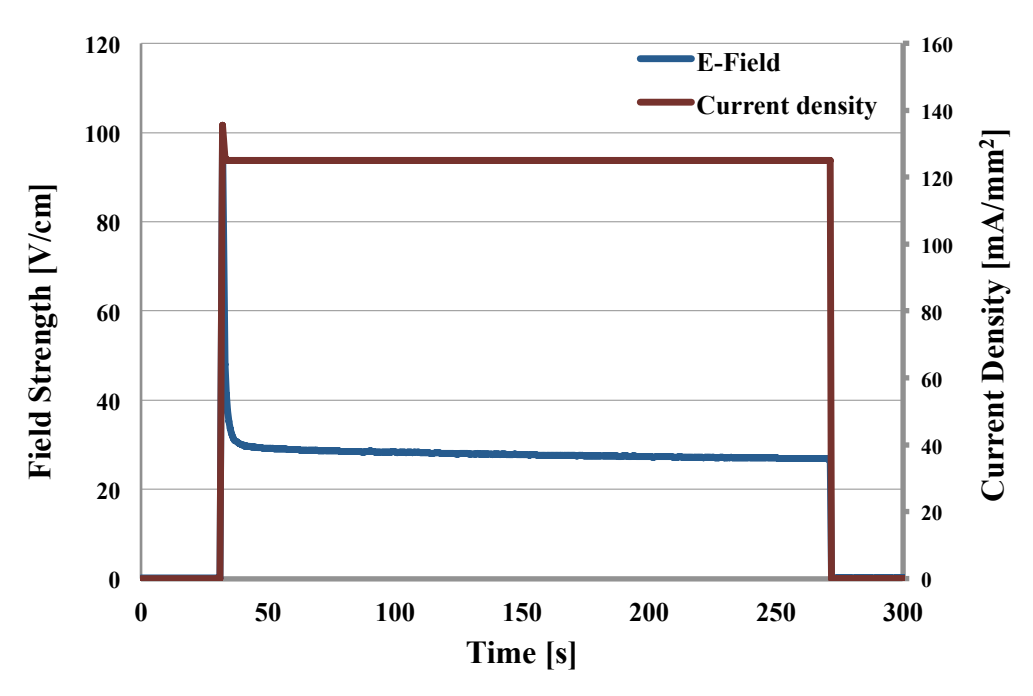


Figure 5. Current and voltage parameter profile during FS of UO₂ (100 V/cm, 125 mA/mm²).

1.3 Application to ATF

Recently, efforts into development of FAS techniques for nuclear fuel fabrication have increased. One technique for increasing the thermal conductivity of uranium dioxide fuel with minimal changes is to fabricate a composite fuel where the constituent phase has a higher thermal conductivity. For example, a UO₂-UB₂ fuel would exhibit a higher thermal conductivity due to the presence of the boride phase. However, these composite fuels may be difficult to manufacture using conventional sintering. High sintering temperatures are required in order to reach high densities, and reactions between the constituents tend to occur during prolonged periods at increased temperatures. For this reason, advanced sintering techniques are proving useful for composite nuclear fuel fabrication. The resulting microstructure of a UO₂-SiC composite sintered using SPS is shown in Figure 6. The technique has also shown to be successful for other high-density fuel composite fabrication, including UN-U₃Si₂ [8].

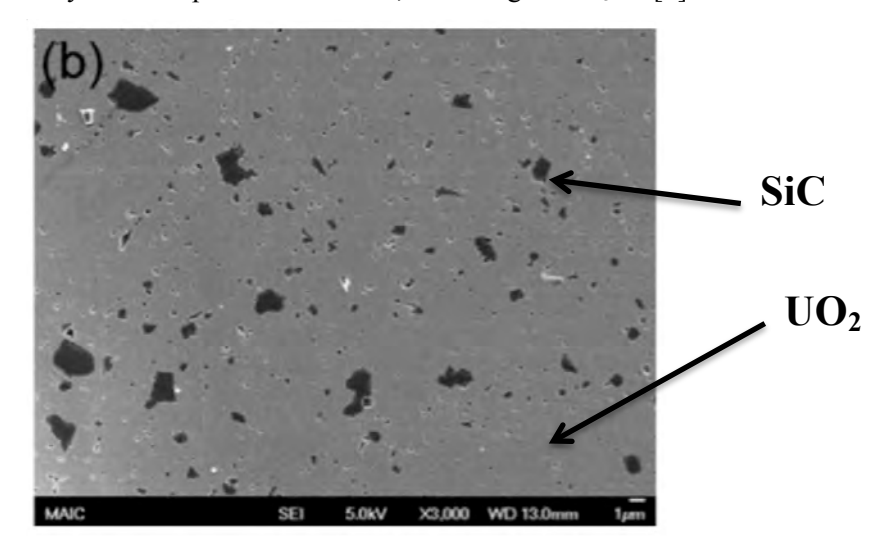


Figure 6. Microstructure of a UO₂-SiC composite sintered using SPS [9].

Although significant research has recently been dedicated to spark plasma sintering of nuclear materials, flash sintering is still widely untouched. In fact, this investigation is the first report on flash sintering of UO₂. Additionally, these results contain the lowest recorded temperature at which flash sintering has occurred (room temperature). Most of the current efforts of research on flash sintering are dedicated towards understanding the effect of the field (and current) on the densification process. Current theories describing the potential effects include electromigration [10], self-cleaning at the grain boundaries [11], and joule heating [12]. The main objective of this in-situ study was therefore to obtain evidence regarding the mechanisms active during flash sintering (temperature, defects, etc). Once these mechanisms are better understood, there will be a better control of densification and a greater likelihood that this technique could eventually be used to sinter nuclear fuel.

2. Experimental

Two separate groups of experiments were completed: dilatometer studies at Los Alamos National Lab (LANL) and in-situ studies at Brookhaven National Lab (BNL). The sample preparation and experimental setup were dependent on the study set, and therefore are described separately in this section.

2.1 Sample Preparation

The uranium dioxide feedstock used in these studies came from AREVA with an as-received oxygen-to-metal (O/M) ratio of 2.16. These materials were characterized by x-ray diffraction (XRD), for phase purity and content. For the initial studies, the feedstock was milled for 15 minutes in a Spex mill with a zirconia ball and vial and then sieved through a 400-mesh sieve. The powder was milled with 1.0 wt% EBS binder for 5 minutes. Following the milling, pellets were pressed to 60 MPa, based on previous work with UO₂, to achieve a reasonable green density of approximately 50-60 %TD. Additionally, larger pellets with 13mm diameter were pressed in order to allow multiple rectangular samples to be cut. The pellets were weighed and measured to determine the geometric density of the materials prior to sintering.

2.1.1 Dilatometer

The pressed and pre-sintered pellet geometry samples were used directly in the dilatometer studies, with a nominal geometry of 4.75 mm diameter and 5.25mm length. The ends of the samples were painted with platinum and they were reduced/oxidized in a TGA to desired stoichiometry, or oxygen-to-metal ratio.

2.1.2 In-situ

Rectangular bar shaped geometry samples were cut from the large 13mm diameter pellets with approximate dimensions of 1mm x 2mm x 7 mmm (Figure 7). This geometry was chosen based on the planned beamline experiments, with the goal of minimizing the width and maximizing the length for scanning. The 7mm length allowed a gauge length of 5mm for the beam to scan. The ends of the samples were painted with platinum and they were reduced/oxidized in a TGA to desired stoichiometry.

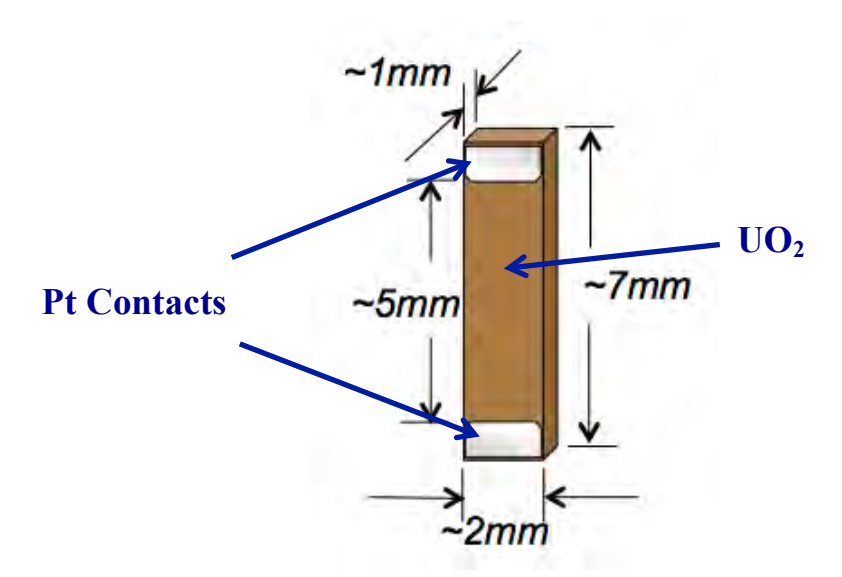


Figure 7. Dimensions of rectangular geometry samples (7mm x 1 mm x 2 mm) used for the in-situ studies.

2.2 Experimental Setup

2.2.1 Dilatometer

The experimental setup includes a Netzsch 402C dilatometer (DIL) furnace and a power supply. The sample was loaded into the DIL and two platinum leads were placed in contact with the sample ends (see Figure 8). The dilatometer measures changes in the length of the material as it is heated, which in turn reflects the densification of the material. A voltmeter was placed in series in order to measure the resistance of the system. This value of resistance proved to be very useful in monitoring the transient behavior of the material during the experiments. The experiments were done under gettered-Ar flowing at 500 mL/min to reduce the possibility of oxidation at high temperatures.

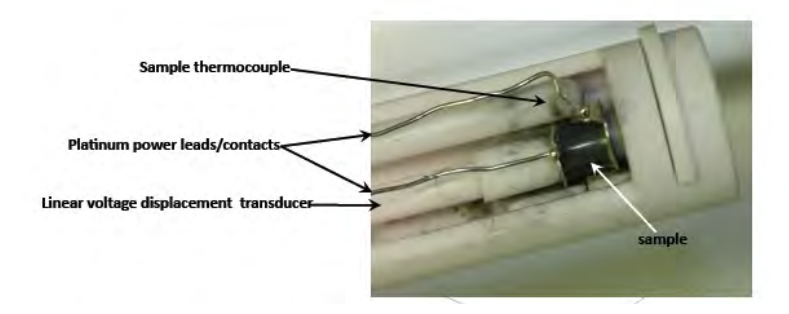


Figure 8. Pellet sample (D = 4.75mm) loaded in dilatometer with leads in contact with ends.

2.2.2 In-situ

The in-situ experimental setup consisted a double quartz tube to contain the sample, a power supply to provide the electrical field, and an oxygen analyzer to monitor purity of argon gas flow. The setup is shown in Figure 9 with an overview of the quartz tube and a zoom view on the sample holder. The sample holder varied between the two separate studies, but both holders had the purpose of providing good contact between the sample and the platinum leads. Lastly, a thermocouple was placed near the sample to record the temperature change of the system.

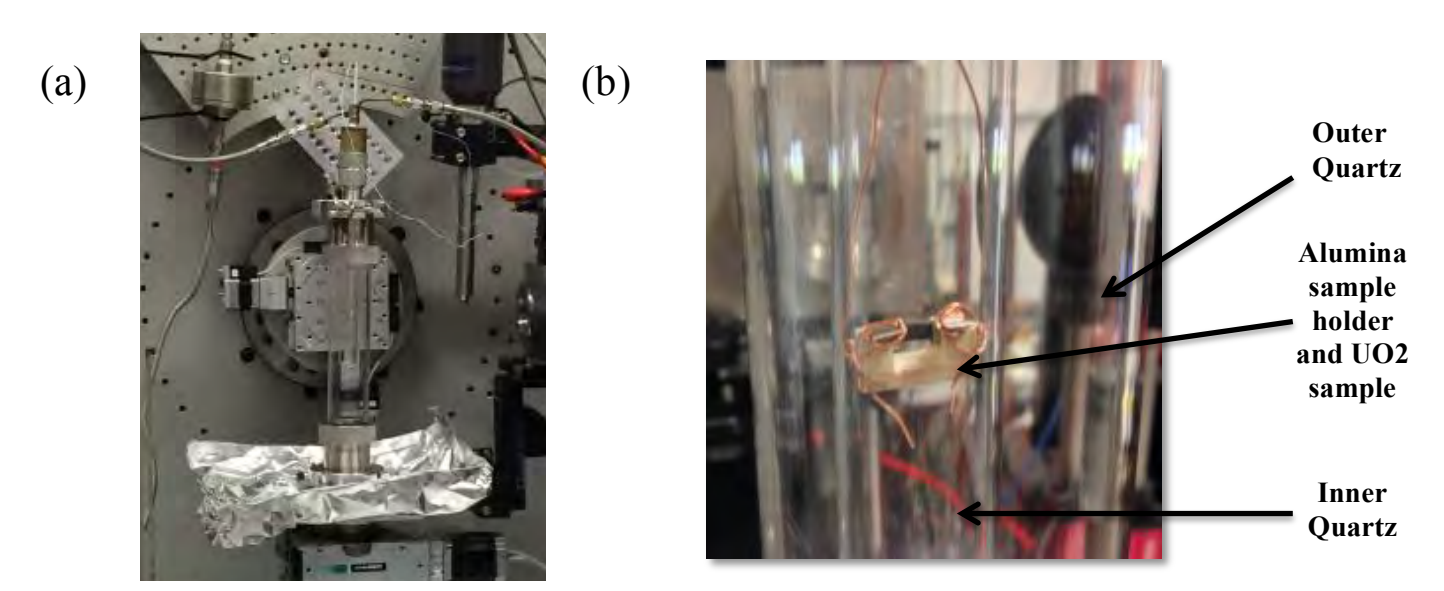


Figure 9. (a) Overview of in-situ experimental setup and (b) close-up of sample loaded.

3. Initial Studies

The initial group of studies was mostly dedicated to optimizing the setup and screening the behavior of pure UO_2 and other systems. These results are summarized briefly here to provide a clear foundation for the in-situ experiments.

3.1 Screening of Key Parameters on UO₂ System

The most obvious parameters that had an influence on the flash sintering behavior were the field strength and current density. The field strength was found to enhance the current runaway behavior, both in terms of time required to run away and acceleration of runaway (Figure 10). Hold time, or the time at which the maximum current is allowed to flow through the sample, had the largest influence on extent of densification. Most of the samples densified in excess of 90% TD required a hold time of 10 minutes or longer.

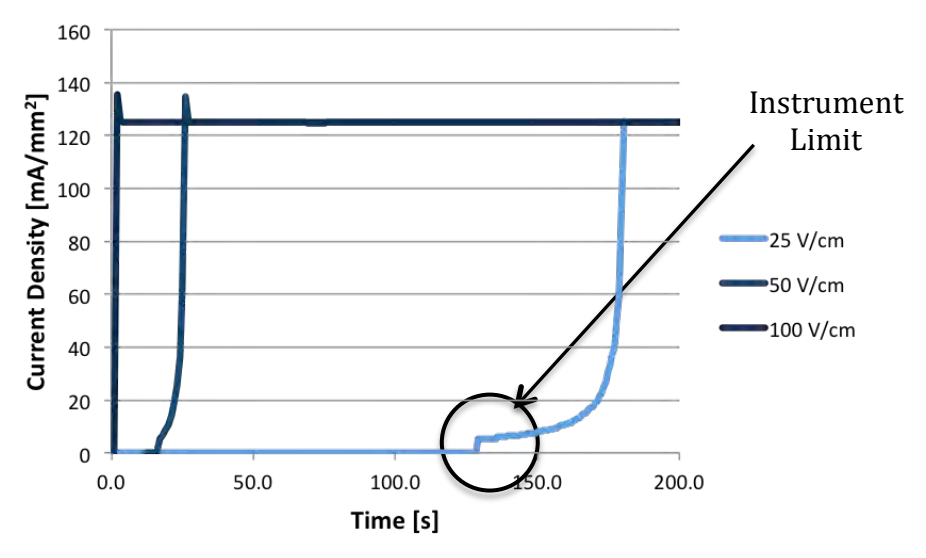


Figure 10. Current runaway for three applied field strengths on $UO_{2.16}$ rectangular sample, showing that the increase in field strength results in an enhancement in the flash behavior.

Table 1 summarizes the parameters that were initially investigated and found to have an influence on material behavior during flash. Some parameters were a surprise in their effect on behavior, including the material starting density (Figure 11) and O/M. A study on the effects of alternating current (AC) and the heating/cooling rates are planned for the future.

Table 1. List of key parameters screened in initial experiments.

Parameter	Range Tested
Field Strength	0-300 V/cm
Current Density	0-700 mA/mm ²
Hold Time	0-10 min
Temperature	27°C-1000°C
Material Starting Density	55%, 70%, 80%, 95%TD
O/M	UO _{2.00} , UO _{2.06} , UO _{2.16}
Atmosphere	Ar, He, Air (no flash)

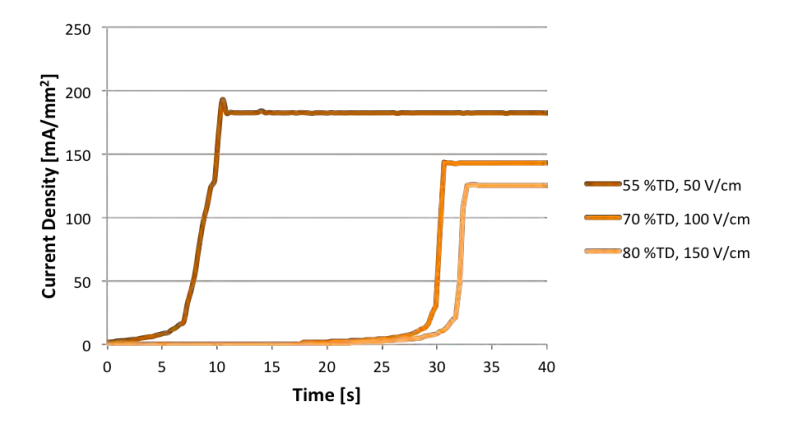


Figure 11. Current runaway for three starting material densities, showing that lower density starting materials enhance the flash behavior.

These initial tests also resulted in a number of discoveries with regard to the experimental setup and data acquisition. For example, the power supply limit for current flow detection was found to be 10.5 mA, meaning no real conclusion on the actual current flow could be drawn for long periods of apparent 'incubation time' (shown above in Figure 10). Since this was a set instrument limit, the incubation phenomenon would have to be investigated further during the in-situ experiments.

3.2 Screening on Composite Systems

Initial screening on composite systems showed that only UO₂ based systems displayed flash sintering behavior. The silicide systems (UN-U₃Si₅, UN-U₃Si₅) tested did not show a current runaway behavior, but instead immediately allowed current flow to occur. The cause for this discrepancy is unknown, but it is speculated now that the high electrical conductivity of these materials is associated with the fact that no flash is observed. It should be noted that only conditions similar to those used for UO₂ were tested, so at this point, flash in these materials cannot be entirely ruled out. The UO₂-UB₂ system showed flash behavior, but it was degraded compared to the pure UO₂ system. These results are displayed in Figure 12.

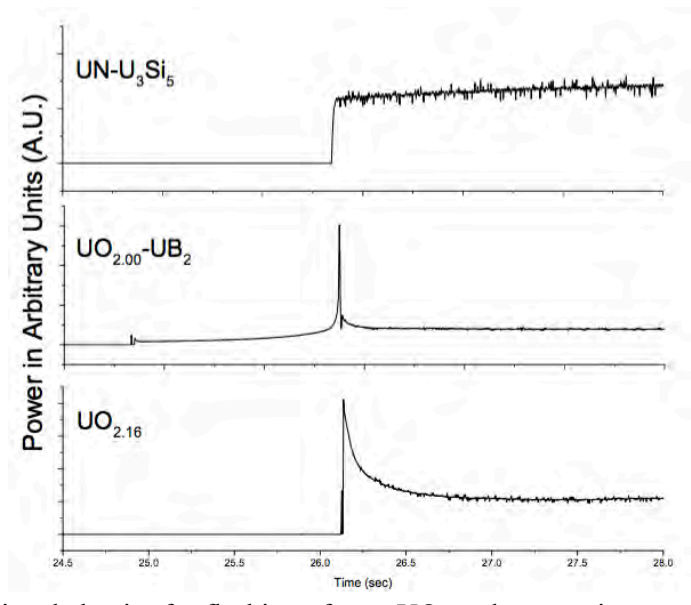


Figure 12. Power transient behavior for flashing of pure UO₂ and composite systems for comparison.

3.3 YSZ Reference Tests

Yttria-stabilized zirconia (YSZ) reference tests were completed as a reference point and for verification of setup, since this material has been widely used in flash sintering experiments [13,14]. Similar behavior was observed (Figure 13) in terms of the field strength and parameter profiles for 8YSZ (8-mol% Y₂O₃ and ZrO₂). However, there was a slight difference in densification, which can most likely be attributed to geometry differences, since the reference case uses a dog-bone shaped geometry instead of pellet geometry.

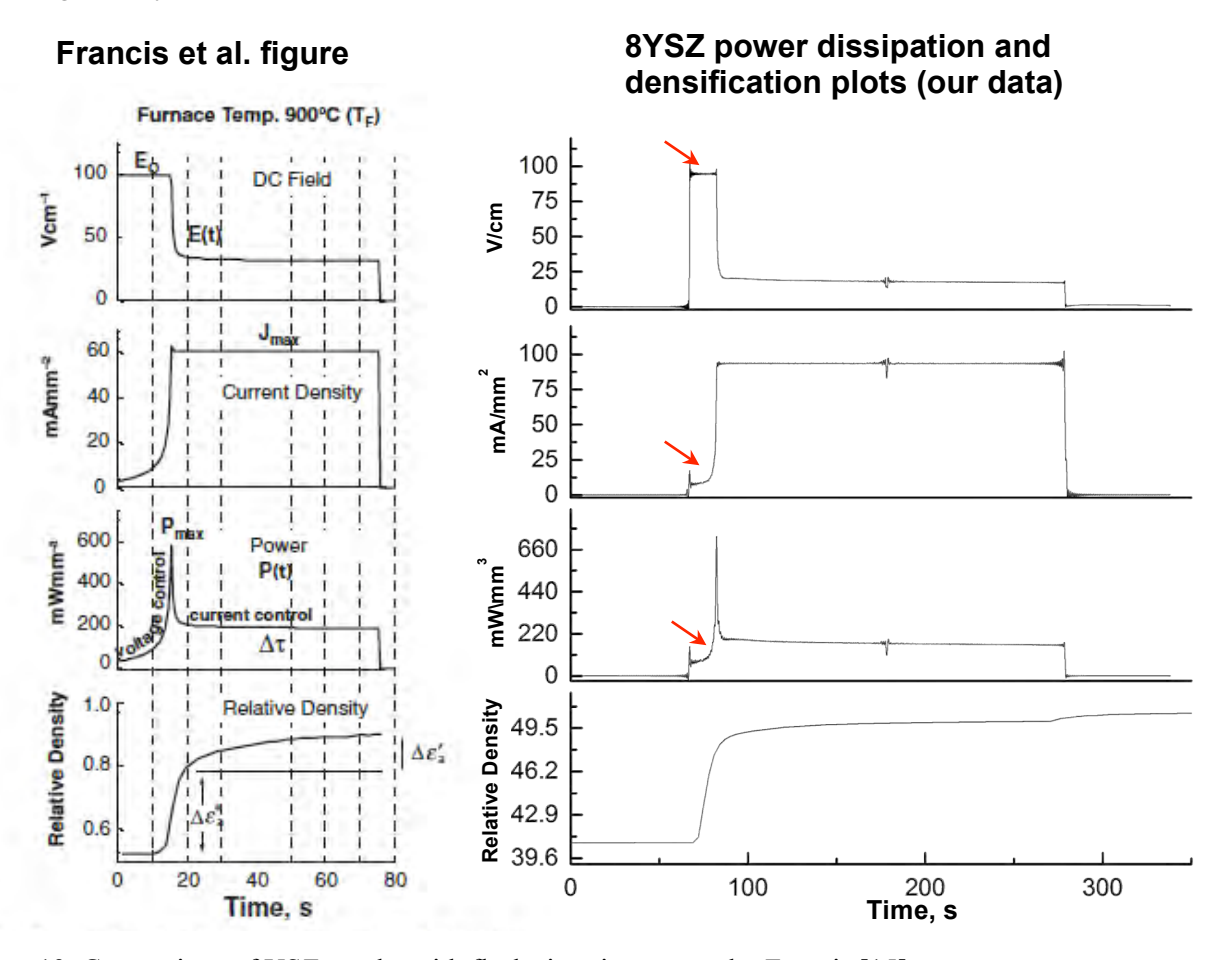


Figure 13. Comparison of YSZ results with flash sintering curves by Francis [15].

4. Current Studies

The new dilatometer studies in this report build off of the results of the initial studies. After establishing a basic understanding of the parameters influencing the flash process, the experimental direction was changed in order to probe how the flash occurs. Various theories exist for explaining the flash phenomena, so the goal of the recent studies is to use experimental evidence to provide results that can validate one or more aspects of these theories.

4.1 Flash/No Flash Zones

One flash parameter of interest was the step time, or time it takes after the field is applied for current to step up to a recorded value, or the moment that measurable current flow occurs. The step time preceding a flash has previously been referred to as 'incubation time' [16]. Step time was measured as a function of system resistance (Figure 14), which could be changed by flashing the sample. The assumption here is that the material resistance is the only thing in the system changing due to sample densification. There is a clear correlation of the step time increasing as the field was decreased. After holding various field strengths, it was found that some lower field strengths do not cause a flash at all. Instead, there is a plateau of the current at a low value (10-30 mA) for an extended period of time (~ minutes). Additionally, it was found that the speed of the flash was directly related with how high the field was above this 'no flash' value. This flash/no flash behavior seems to be direct evidence that there is a system containing instability points, where the current will runaway rather than plateau.

Another interesting find was that the fluctuating room temperature changed the material resistance from 0.55 k Ω to 0.43 k Ω (27°C to 28.5°C). This change over a few degrees highlights the strong negative temperature coefficient (NTC) of resistivity of uranium dioxide. The NTC plays a very important role in the thermal runaway model, which describes instability in heating due to the changing resistance and low thermal conductivity of the material.

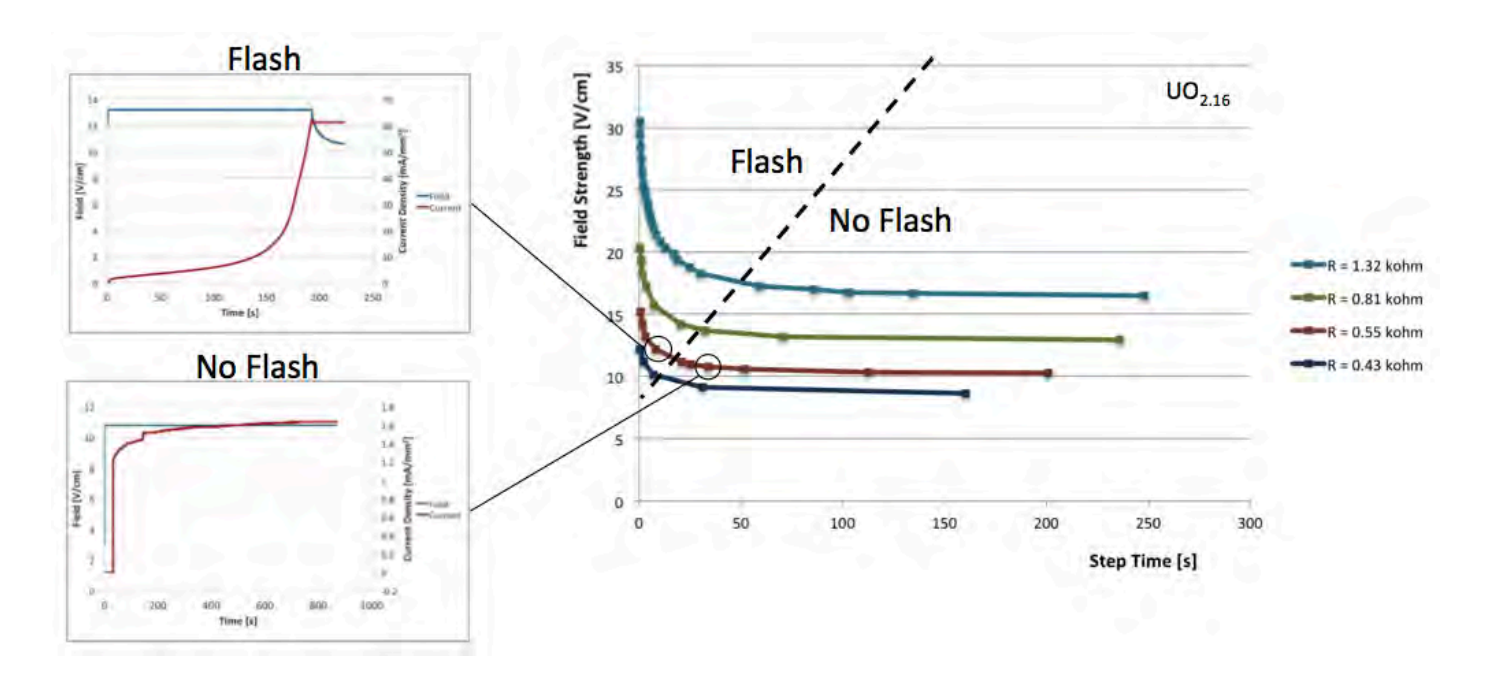


Figure 14. Field strength vs. step time for varying material (system) resistance.

4.2 Lead Orientation Effects

The effect of lead orientation was measured by alternating anode and cathode leads on the sample and measuring the step time before changing to the next field strength. The results are in Figure 15, and show that there is no polarity hysteresis observed in step time. This may suggest a reversible phenomenon that is not heavily dependent upon ion migration.

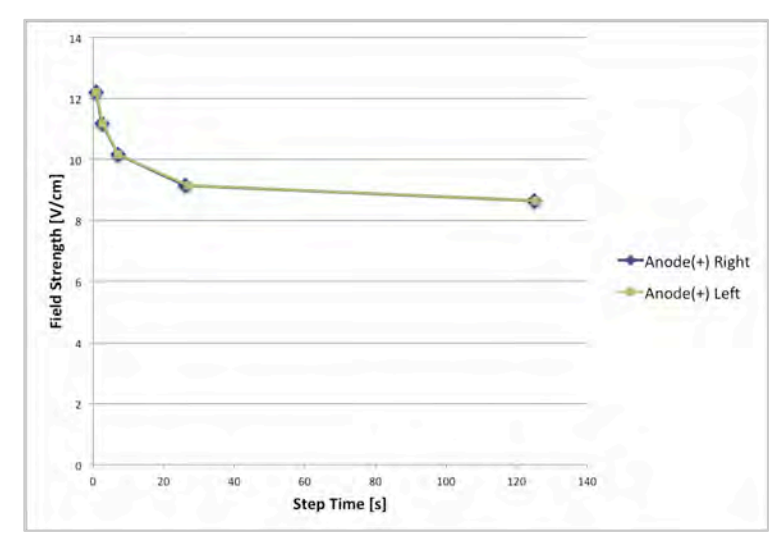


Figure 15. Step time results for alternating anode and cathode leads on a UO_{2.16} rectangular sample.

4.3 Critical Field Studies

There are typically two methods to determine the critical field at flash, or Ecrit:

- (1) Voltage constant/Temperature ramp
- (2) Temperature constant/Voltage ramp

In both methods, the current flow is recorded and the voltage/temperature combination where a flash occurs is taken as the critical field. The temperature ramp is typically around 10°C/min [17], but the appropriate voltage ramp rate was initially unknown. For this reason, multiple voltage ramps were tested before using method (2) for the critical field studies.

4.3.1 Voltage Ramp Rate

The effect of voltage ramp on critical field at flash was foreseen due to the resistance changes that will occur in the material during the voltage ramp up time (sample heating). The goal was to achieve a voltage ramp rate that was essentially infinite in order to minimize these changes. Figure 16 summarizes the results of six different ramp rates for three system resistances. As the ramp rate increases, the field strength required for current flow to occur reaches an asymptotic value. Additionally, the time required for current flow to occur approaches zero. The rate was cutoff at 1 V/s since the lowest acquisition time for the Labview program is 300ms. Therefore, 1 V/s was chosen as the rate that would approach infinity while still allowing an acceptable amount of data acquisition.

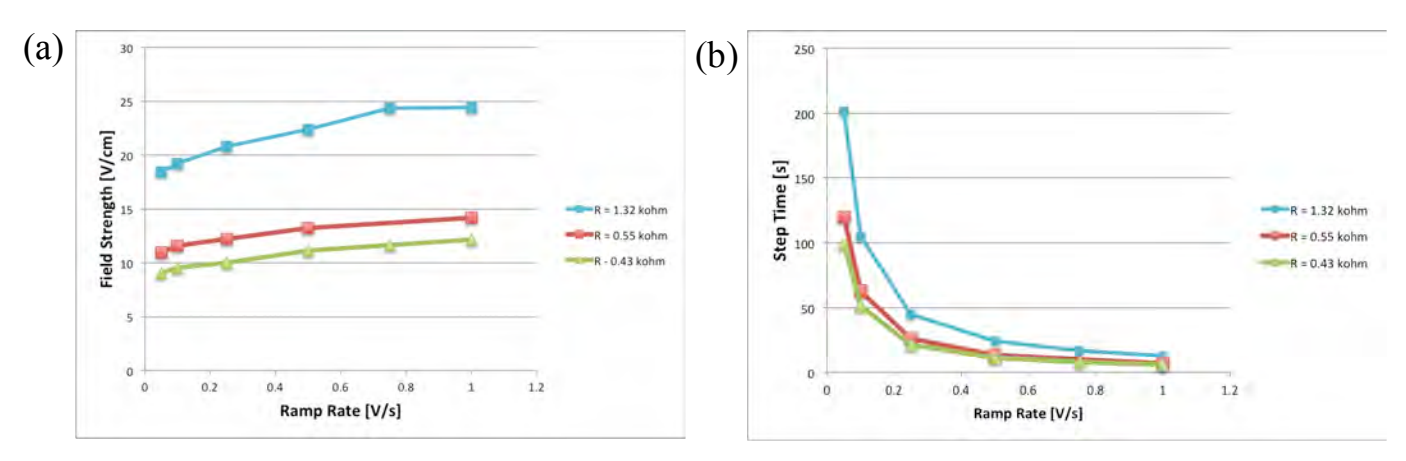


Figure 16. Influence of voltage ramp rate on (a) field strength at flash and (b) step time of UO_{2.16} sample.

4.3.2 Critical Field Results

The critical field for $UO_{2.00}$ was determined by using the ramp rate of 1 V/s on a sample with starting density 95%TD, shown in Figure 17. These results will be compared to an existing thermal runaway model in order to provide verification between experiment and model. This model is explained in further detail in the next section.

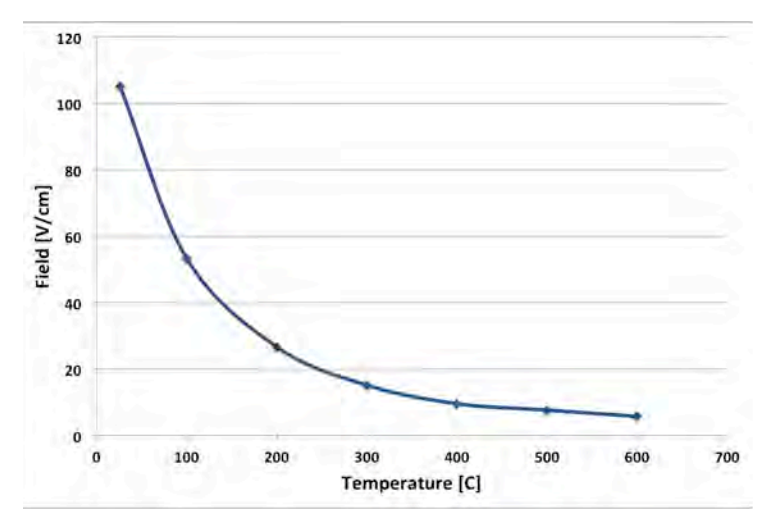


Figure 17. Critical field results for UO_{2.00} with 1 V/s voltage ramp at isothermal temperature.

4.3.3 Model Comparison

Over the past year, a number of models have been produced to predict flash sintering, most of which are based on the theory of thermal runaway from joule heating. Due to the close match of these models to experimental results, there is now a wide agreement that thermal runaway plays a large part in the flash occurrence [18.19]. A PhD student at Technical University of Hamburg created the model that will be used for comparison with these experiments. It describes flash sintering using bifurcation theory stability analysis on the thermal runaway model [20]. The positive feedback of thermal runaway is described in Figure 18. This feedback mechanism is expected to occur until either the pre-defined current limit is reached or the sample fails.

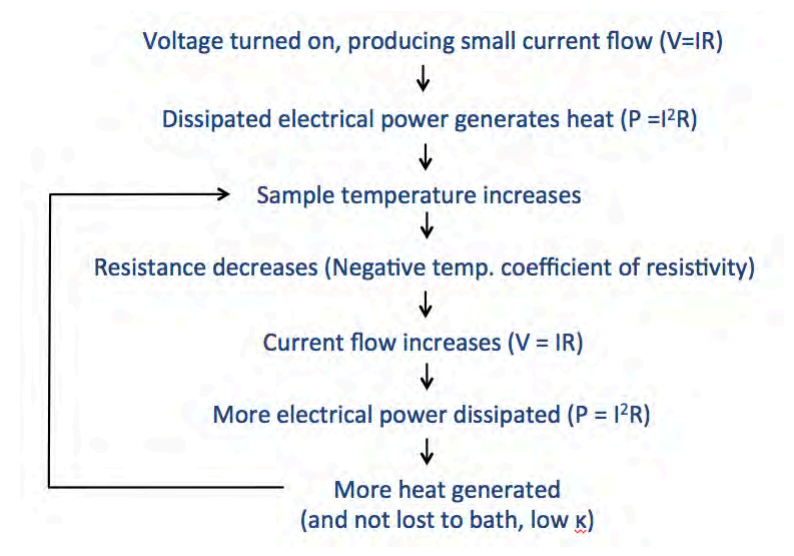


Figure 18. Flow-chart describing thermal runaway process.

The specific model contains two parts: a heat equation to describe thermal runaway and an activation energy kinetic equation to describe densification. Bifurcation theory is then used to analyze the stability of the system. The information experimentally determined for use in the model includes the electrical conductivity (resistivity variance with temperature) and the densification (sintering kinetic parameters with temperature). The electrical conductivity data can be extracted from the critical field results and the densification data is determined in the dilatometer with only the application of temperature. The stability analysis results in a comparison between the experiment and model for the critical field at flash as a function of temperature. An example of this comparison is shown in Figure 19.

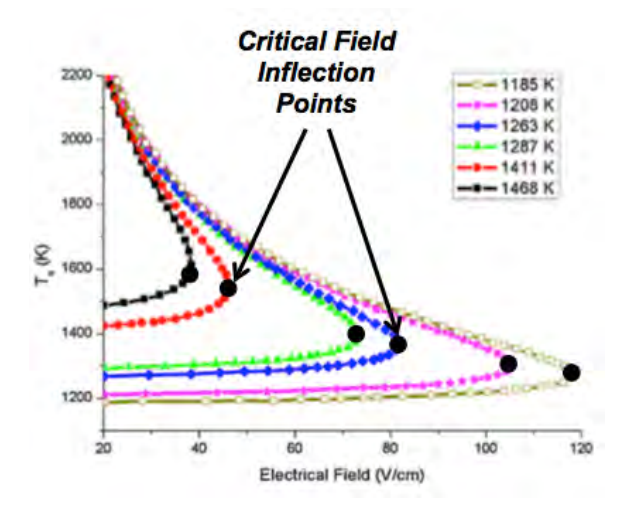


Figure 19. Example of bifurcation theory used to determine critical field points [20].

5. In-situ Studies at Brookhaven NSLS-II

Two separate groups of experiments were done at Brookhaven National Lab's NSLS-II XPD-I beamline. The results analyzed the phase and lattice parameter evolution during flash of UO_{2.00}, UO_{2.16}, and UO_{2.23}. Although each set of experiments had their own goals, the overall objective was to improve the understanding of mechanisms active during flash sintering (phase content, temperature, defects, and strain).

5.1 XPD-I Beamline

XPD-I is an x-ray powder diffraction beamline that offers the ability to collect structural data at high energies, providing the ability to structurally characterize materials in-situ during experiments. It can do this because of the high energy/flux, rapid data acquisition, and high resolution of patterns. The following in-situ experiments were done with a beamline energy of 64.67 keV, beam size of 200 x 200 μ m², and collection time of 0.1s with the beam centered on the sample. Figure 20 shows a photo at the beamline of the equipment setup for the experiments. The phase identification was based on:

- Number of peaks (phases, impurities)
- Peak shift/position (O/M, lattice parameters, temperature effects)
- Peak width (defects, crystal structure, grain size)

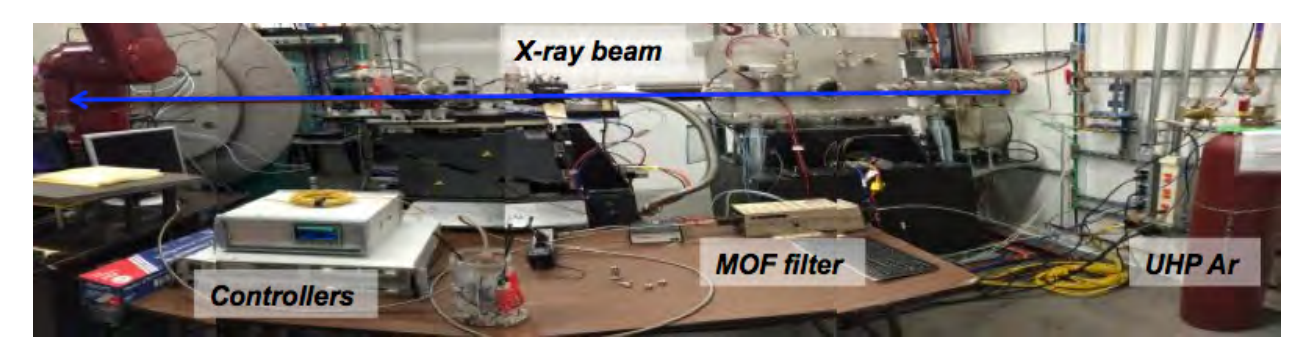


Figure 20. View of XPD-I beamline with experimental equipment.

5.2 First Study Set Results – Field Strength and Current Density

The first group of experiments had the objective of probing the field strength and current density effects on phase evolution. Dilatometer studies showed that both parameters had a significant effect on the flash behavior, but the exact effect was still unknown.

5.2.1 Experimental

As stated in section 2.1.2, fabricated rectangular bars were used in the in-situ experiments. The geometry for the first batch of experiments was 1mm x 2mm x 7mm. The ends of the sample were constrained by clamping with platinum leads in an alumina holder, illustrated in Figure 21. The samples had an average starting density of 55% TD and starting O/M of 2.12. The ends were dipped in platinum and before clamping with the platinum leads. There was a 5mm gauge section for which the beam could collect data from.

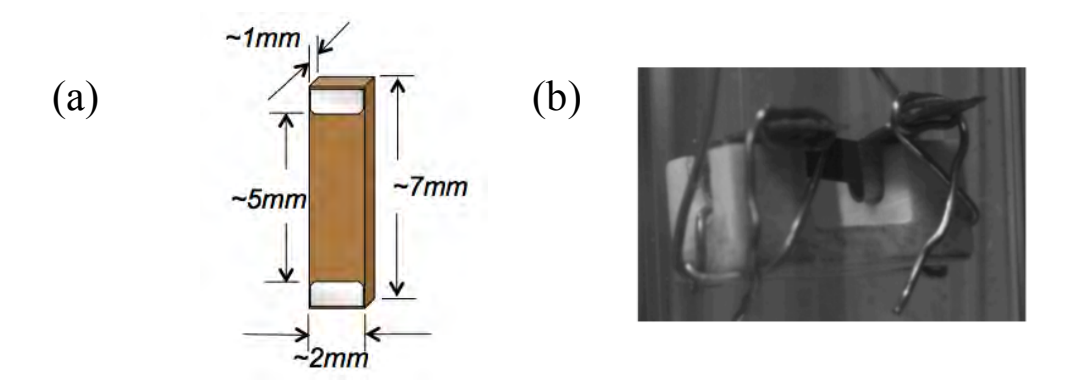


Figure 21. In-situ (a) sample geometry and (b) sample clamped and loaded into alumina holder.

5.2.2 Low Field/Low Current

A 25 V/cm field was applied to a $UO_{2.16}$ sample and it was flashed to allow a current density of 50mA/mm^2 to flow for 300s. The voltage and current parameter profile is shown below in Figure 22.

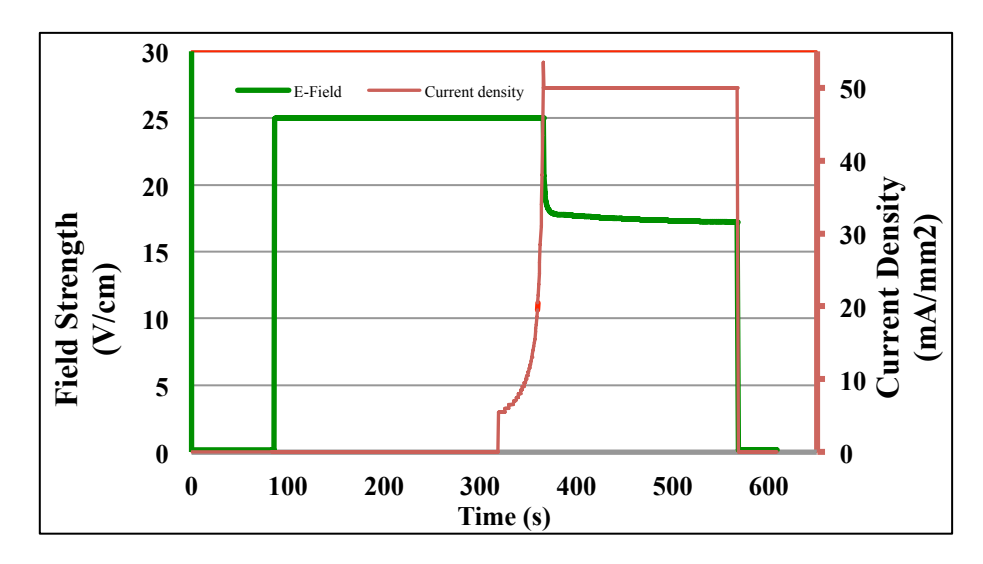


Figure 22. Voltage/current parameter profile during low voltage/low current flash of UO_{2.16}.

5.2.2.1 Lattice parameter evolution UO_{2.16}

The lattice parameter evolution of $UO_{2.16}$ during the low field/low current induced flash is shown in Figure 23. Since the sample starts at approximately 50% UO_2 and 50% U_4O_9 , the evolution of both lattice parameters is shown. The first observation is that there are changes in both lattice parameters immediately after the field is applied and well before the flash occurs. These initial changes in the lattice parameter are also opposing, with the UO_2 expanding and the U_4O_9 contracting. The cause for the opposing trends at this time was unknown. Afterwards, both parameters expand during flash, which is to be expected. The U_4O_9 does not convert, indicating that the temperature during flash did not exceed 1073K based on extrapolations from published binary phase diagrams from the U-O system.

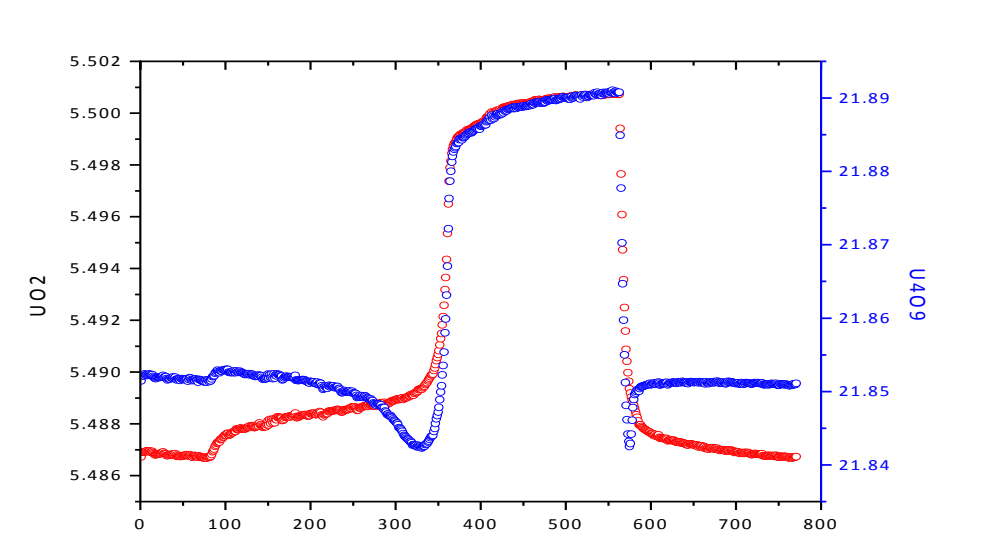


Figure 23. Lattice parameter changes for UO_2 (red) and U_4O_9 (blue) during low voltage/low current flash of $UO_{2.16}$.

Time (s)

5.2.2.2 Phase Evolution UO_{2.16}

The phase evolution during the flash was analyzed in order to track U_4O_9 conversion, which could reflect the temperature reached during the experiment. These results are summarized in Table 2. The lattice parameter values show little change in the final structure after the flash, signifying no clear defect residual strain. However, there was a slight change in the phase fraction, meaning some of the U_4O_9 did convert to UO_2 .

Table 2. Phase content and lattice parameter values for before and after low voltage/low current flash of $UO_{2.16}$.

Before	a (Å)	Strain (%)	Grain size (nm)	Fraction (%)
UO ₂	5.487	0.015 (0.003)	181 (28)	40.6 (0.8)
U ₄ O ₉	21.853	0.019 (0.004)	139 (24)	59.4 (0.8)
After				
UO ₂	5.487	0.022 (0.001)	180 (15)	44.25
U ₄ O ₉	21.850	0.029 (0.004)	137 (24)	55.8 (0.8)

5.2.3 High Field/High Current

A 100 V/cm field was applied to a $UO_{2.16}$ sample and it was flashed to allow a current density of 125mA/mm^2 to flow for 30s. The voltage and current parameter profile is shown below in Figure 24.

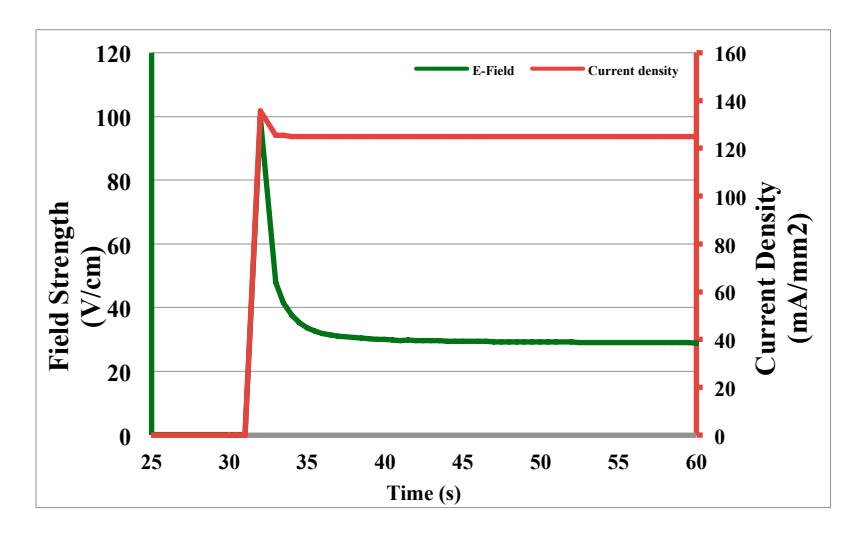


Figure 24. Voltage/current parameter profile during high field/high current flash of UO_{2.16}.

5.2.3.1 Lattice parameter UO_{2.16}

Figure 25 shows the lattice parameter evolution of $UO_{2.16}$ during the high field/high current induced flash. Both parameters expand rapidly until the U_4O_9 is completely converted to $UO_{2.00}$ by the end of the flash. Using the lattice parameter values, the peak temperature was estimated at 1500 K, so the phase conversion is most likely temperature induced.

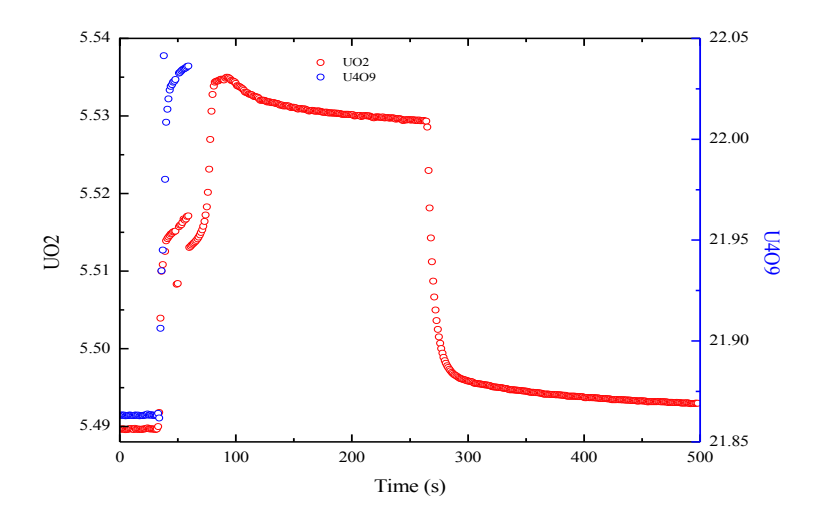


Figure 25. Lattice parameter changes for UO_2 (red) and U_4O_9 (blue) during low field/current flash of $UO_{2.16}$.

7/01/2016

5.2.3.2 Phase Evolution UO_{2.16}

Table 3 shows the initial and final values for phase content during the flash, confirming that all of the U_4O_9 was converted to UO_2 . The oxygen-uranium phase diagram is shown below in Figure 26 to display how complete conversion of $UO_{2.16}$ would occur, namely that a temperature of 1000K should be exceeded. Figure 27 shows the peak change at each stage during the flash and the associated phase changes. There is some slight broadening that occurs initially, which may indicate structural change. Unfortunately, the role of defects could not be identified since they are so strongly tied to the temperature.

Table 3. Phase content and lattice parameter values for before and after low voltage/low current flash of $UO_{2.16}$.

Before	a (Å)	Strain (ε ₀)	Grain size (nm)	Fraction (%)
UO_2	5.486	0.015 (0.003)	185 (15)	35 (0.8)
U_4O_9	21.851	0.038 (0.004)	122 (20)	65 (0.8)
After				
UO_2	5.489	0.013 (0.001)	192 (15)	100

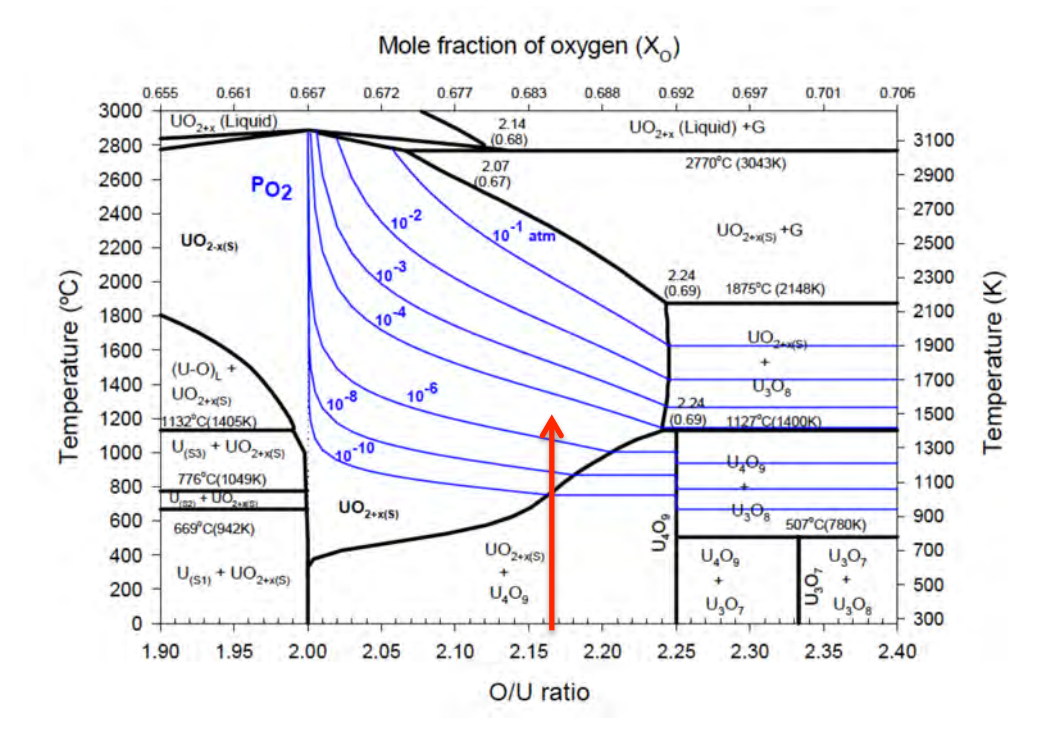


Figure 26. Oxygen-Uranium phase diagram, highlighting how conversion would occur for UO_{2.16} [21].

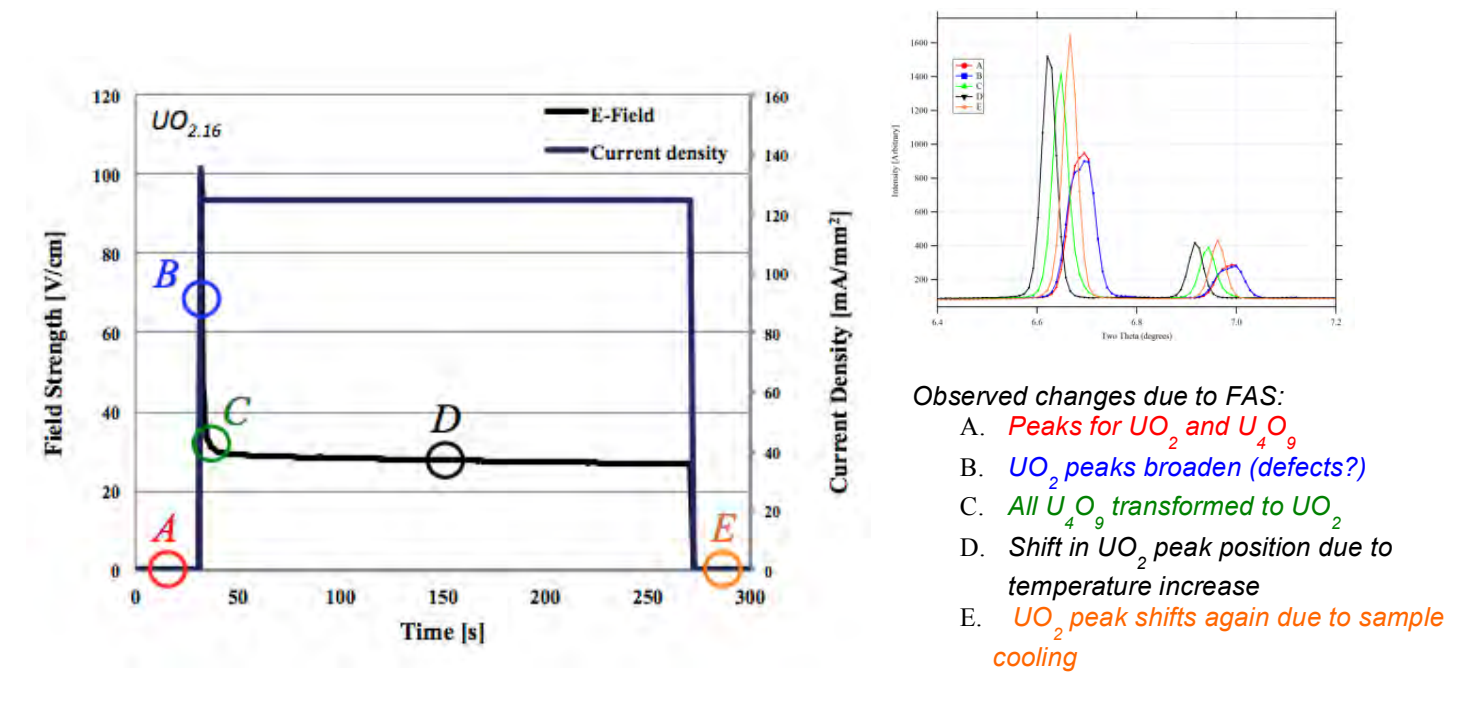


Figure 27. Parameter profile with changes in peaks sequentially labeled for high voltage/high current flash of UO_{2.16}.

5.3 Second Study Set Results – Incubation Time and Scanning

The second set of experiments had the objectives of examining the incubation time behavior of the material and determining whether ion migration was occurring. The former was completed by holding and flashing samples at very low fields and the later was completed by continuously scanning the sample during the experiment.

5.3.1 Experimental

Rectangular samples were used again, but there was a slight change in geometry, with the samples cut to 3mm x 7mm x 1mm. The purpose of the change in width from 2mm to 3mm was to create more area for the beam to scan the samples in the scanning experiments. The most significant change experimentally between the first and the second set of experiments was the addition of a spring-loaded sample holder, pictured in Figure 28. Since good contact with the leads was maintained with the spring, only the very ends of the samples had to be painted with platinum.

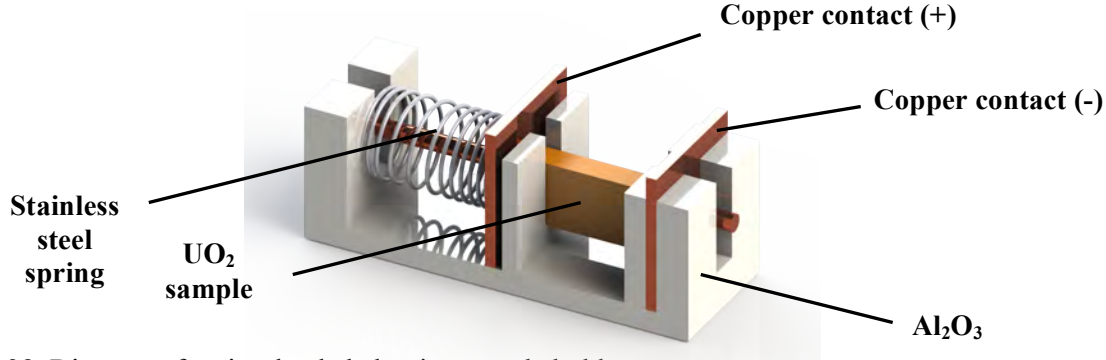


Figure 28. Diagram of spring-loaded alumina sample holder.

Three different O/M samples were fabricated: UO_{2.00}, UO_{2.16}, and UO_{2.23}. The purpose of using samples with differing stoichiometry was to gain a greater insight on the phase changes occurring during the experiments, giving a better idea of temperature reached.

5.3.2 Incubation Time

An example of incubation time is shown below (Figure 29) and typically occurs for lower fields. Therefore, in order to explore this time period, a low flash field had to be chosen for each individual sample. The method to determine this specific field was established during the dilatometer studies. First, the voltage was ramped at 1 V/s until the current stepped up to a low value (~10.5mA). The field at which this step of current occurred was taken as a low field that will cause a flash. This fact that the sample would flash at this field was discovered from experience during the dilatometer ramp rate studies. It is important to clarify here that the magnitude of the field will vary from sample to sample according to stoichiometry, because the resistivity of uranium dioxide is dependent upon oxygen content, or O/M.

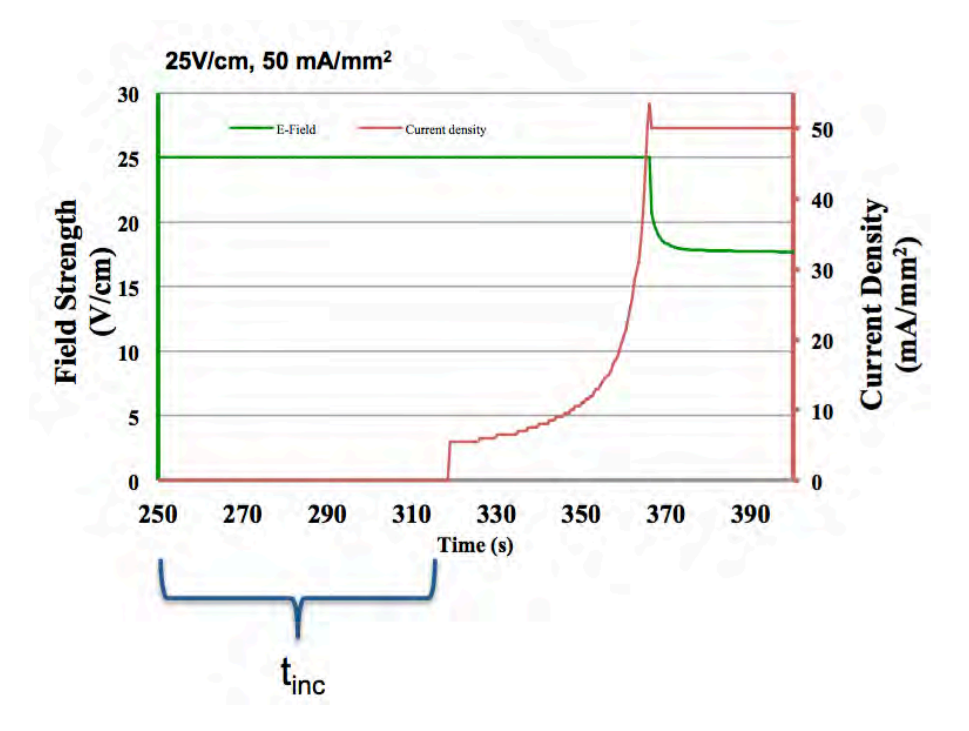


Figure 29. Example of flash parameter profile with incubation time.

5.3.2.1 Lattice Parameter UO_{2.00}

A field of 137 V/cm was applied to a stoichiometric sample, in order to induce a slow flash and observe the lattice parameter change during the time before measureable current flow. Once the flash occurred, the current was held for 30s at a current density of 100mA/mm^2 . Figure 30 shows the change in the lattice parameter during the first 200s. The total experiment time was 1200s and the actual change in the lattice parameter before and after was 4.45926 Å to 4.45881 Å. These close values indicate little structural change occurring due to the flash. The UO_2 lattice parameter only expanded, as is expected with an increase in temperature. However, of greater interest is the fact that the parameter begins expanding before current flow is measured (area highlighted in red). The estimated change in temperature during this incubation time is $\sim 250^{\circ}\text{C}$ using the linear coefficient of thermal expansion (CTE) of 9.8E-6. While this estimate seems high, there is clear evidence that changes are occurring in the lattice, either attributed to current flow that is too low to detect or to field effects.

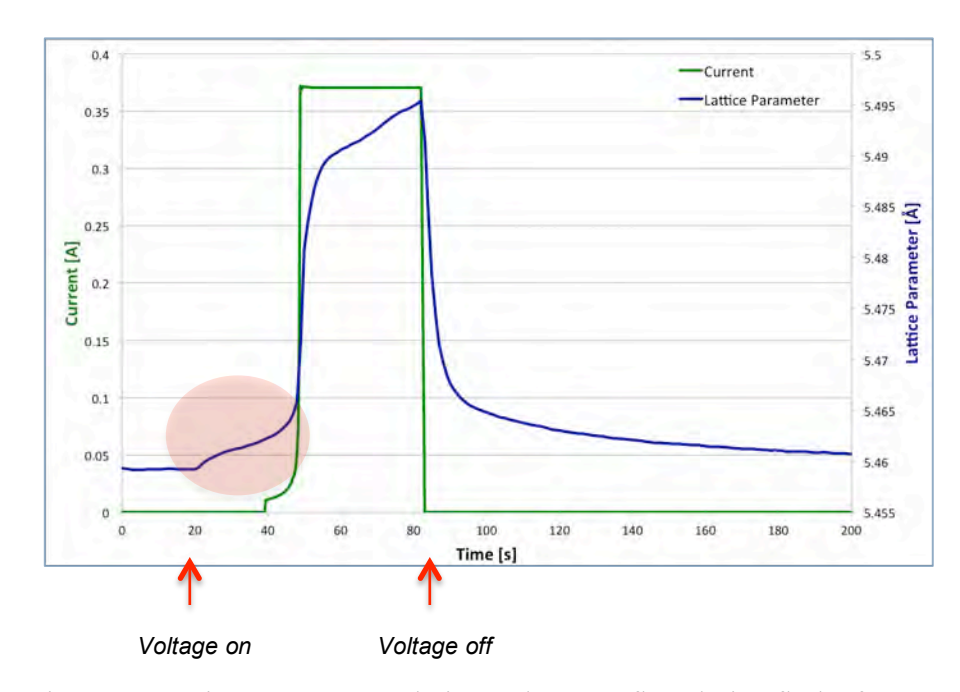


Figure 30. Lattice parameter evolution and current flow during flash of UO_{2.00}.

5.3.2.2 Lattice Parameter UO_{2.23}

A field of 10 V/cm was used to cause a slow flash in the $UO_{2.23}$ sample, with a current density of 100mA/mm^2 held for 30s. Figure 31 shows the lattice parameter evolution during the first 400s of the experiment. The starting lattice parameter was 4.45205 Å and the ending lattice parameter (after 1200s) was 4.45176 Å, meaning there was little permanent change in the structure.

One interesting observation was that the U_4O_9 initially expands and then contracts (highlighted in red in Figure 31), as was seen in the first set of in-situ experiments. After looking into phase transformations of U_4O_9 , it was found that at around 75°C there is a re-structuring phase transition that occurs. Evidence of this transition is shown in Figure 32. This transition likely gives the best indication of the sample temperature during the experiment. The problem with estimating sample temperature in these experiments is two-fold, the thermocouple can only be placed so close to the sample and uranium dioxide has a poor thermal conductivity. For this reason, the thermocouple temperature cannot be expected to accurately reflect the true sample temperature. The structure behavior is much more likely to provide reliable information about the sample temperature.

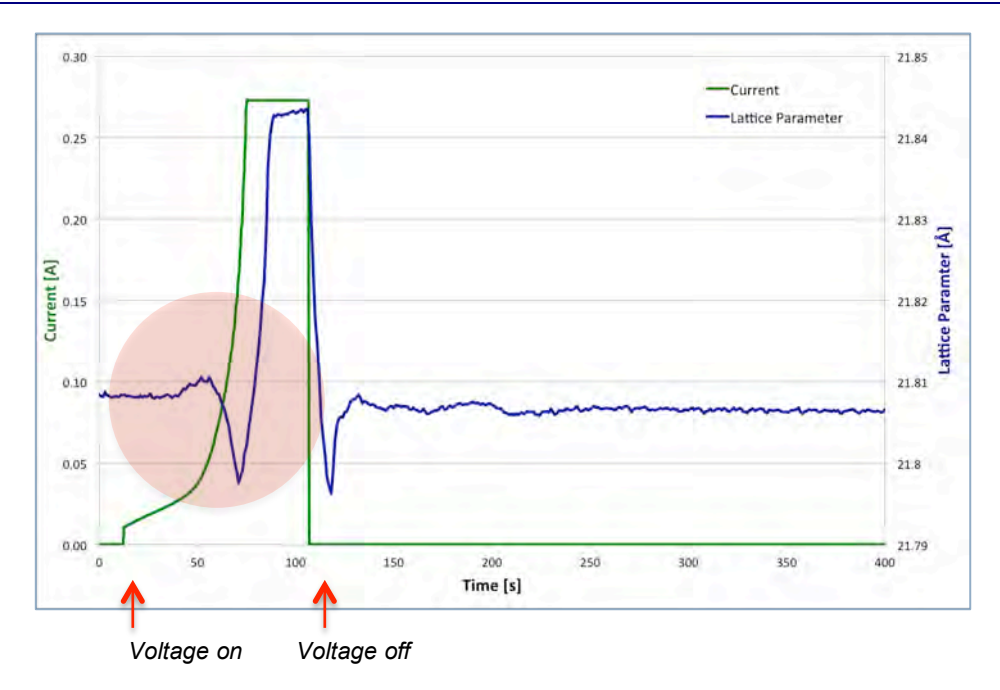


Figure 31. Lattice parameter evolution and current flow during flash of UO_{2.23}.

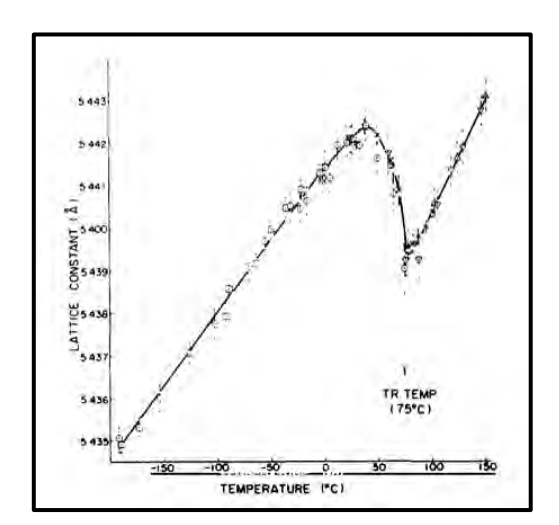


Figure 32. Evidence of a phase transition occurring in U₄O₉ at 75°C [22].

5.3.3 Scanning Experiments

Studies were conducted to investigate the existence of any ion (oxygen) migration. To do this, the sample was continuously scanned at five points during experiments. Experiments with prolonged incubation times and with a flash were done on different stoichiometries ($UO_{2.00}$, $UO_{2.23}$). The comparison of the lattice parameter from one end of the sample to another should give an idea whether oxygen is migrating towards the cathode due to the field strength. While the experiments are complete, the results are still in the process of being analyzed by the beamline scientists at BNL, so they cannot be summarized yet in this report.

6. Summary of Key Observations to Date

The results in this report are significant due to their novelty – the discovery that flash sintering is possible on uranium dioxide and that it will occur at temperatures as low as room temperature. Additionally, some key observations have been made that contribute to both knowledge of the mechanisms active during flash sintering and provide information to guide further studies on the material. These will be summarized in this section according to their experimental setup (dilatometer or in-situ).

6.1 Dilatometer Studies

- Flash sintering of uranium dioxide was achieved at temperatures from as high as 1000°C down to room temperature (26°C)
- At 600°C, greater than 90%TD was achieved by flashing at high fields and allowing current to flow through pellet geometry, and resulted in grain size greater than 10 µm.
- Flash sintering is a function of multiple parameters, including applied voltage, system (material) resistance, temperature, oxygen-to-metal ratio, and starting material density.
- There is no polarity hysteresis observed in step time (time to measurable current flow), suggesting a reversible phenomenon not heavily dependent on ion migration.
- The voltage ramp rate affects the critical field at flash, with approximately 1 V/s simulating an infinite ramp rate.
- Not all measurable current flow leads to flash, so there exists some threshold at which flash will or will not occur.
- For ATF composites, flash sintering has only been demonstrated in UO₂-based systems.

6.2 In-situ Studies

- In-situ flash sintering of UO_{2.00}, UO_{2.16}, and UO_{2.23} successfully performed at BNL's NSLS-II.
- In-situ XRD experiments were used to observe lattice parameter evolution and phase change during flash sintering.
- High field/high current density samples show complete conversion of UO₂ to U₄O₉, indicating that temperatures in excess of 1000K were reached.
- Low field/low current density samples flash but do not show complete phase conversion, meaning much lower temperatures.
- Expansion of lattice parameter was observed during UO_{2.00} flash, but afterwards lattice returns to initial value (no serious defect accumulation).
- Initial contraction observed in UO_{2.23} flash (corresponding to known U₄O₉ phase transition), but also returns to initial state.
- All results point to the fact that the temperature effect on lattice parameter seems to dominate during flash sintering.

7. Recommendations/Path Forward

All of the observations above have paved the way for some recommendations as to what the path forward with UO₂ flash sintering experiments should be. The clear first goal is to complete the current critical field studies and to couple modeling with these results. This will allow for a greater understanding of the flash behavior according to stoichiometry and will validate a model that can be expanded upon in the future. The critical field studies for samples with three different O/M ratios (UO_{2.00}, UO_{2.08}, UO_{2.16}) will be done and the results compared to the thermal runaway model. These results on stoichiometry may give information on the best starting O/M of the material in order to optimize the flash sintering process.

The next step after this initial report on flash sintering of UO₂, as far as dilatometer studies, would be to use this information to start to control densification of the material. This would have to be done by experimental iterations using the various parameters. For example, different fields would be applied and densification effects from each field recorded. Then for each field, current density would be altered to look at this effect. Ideally, this is the data that will be most useful in using this technique of sintering to actually fabricate fuel in the future.

Additionally, a further study on flash sintering of composites may be required, since the current results have only been tested for conditions that are effective on UO_2 . However, at this point, a general conclusion would be that spark plasma sintering is much more successful than flash sintering for non UO_2 -based composites. The recommendation would therefore be to use SPS to fabricate these materials and continue to pursue flash sintering for UO_2 .

The in-situ studies have given some indication of the temperature reached before, during, and after the flash. They show that the field strength and current flow will influence the sample temperature reached, which is promising since it shows that these parameters could be altered to sinter to specific conditions. Methods for decoupling the defect and temperature effects on sintering behavior are still ongoing, with some form of atomistic modeling likely to be used to prove the difference. The results regarding ion migration, once fully analyzed, will be very valuable towards verifying or disproving that theory.

In conclusion, flash sintering is an innovative method of sintering, which could one day allow for a more economic fabrication of materials or even the production of materials with a tailored microstructure. This current research dedicates to the general expanding knowledge of mechanisms active during flash sintering and contributes results that are valid for potentially using the method to sinter nuclear fuel.

8. References

- 1. V.S. Yemel'yanov and A.I. Yevstyukhin, Chapter 8 Compounds of Uranium with Oxygen, The Metallurgy of Nuclear Fuel, Pergamon, 1969, 118-140.
- 2. N. Fuhrman, L.D. Hower, JR. and R.B. Holden, "Low-Temperature Sintering of Uranium Dioxide," Journal of American Ceramic Society, 46 (1963) 114–121.
- Z. A. Munir, D.V. Quach, M. Ohyanagi, Electric Field and Current Effects on Sintering, Sintering Mechanisms of Convention Nanodensification and Field Assisted Processes, Springer, 2013, 137— 150.
- 4. P. Guyot, V. Rat, J.F. Coudert, F. Jay, A. Maître, N. Pradeilles, "Does the Branly effect occur in spark plasma sintering?" Journal of Physics D: Applied Physics, 45 (2012) 1-4.
- 5. L. Ge, G. Subhash, R. H. Baney, J. S. Tulenko, E. McKenna "Densification of uranium dioxide fuel pellets prepared by spark plasma sintering (SPS)." Journal of Nuclear Materials, 435 (2013) 1-9.
- 6. H. Yoshida, Y. Sakka, T. Yamamoto, J. Lebrun, R. Raj, "Densification behavior and microstructural development in undoped yttria prepared by flash-sintering," Journal of European Ceramic Society, 34 (2014) 991-1000.
- 7. D. Byler, Report on field assisted sintering of high uranium density ceramic fuels, assessing voltage and current effects, Milestone Report, Fuel Cycle Research and Development, 2015.
- 8. K. Johnson, A.M. Raftery, D.A. Lopes, J. Wallenius, "Fabrication and microstructural analysis of UN-U3Si2 composites for accident tolerant fuel applications," Journal of Nuclear Materials, 477 (2016), 18-23.
- 9. C. Yeo, S., et al. (2013). "Enhanced thermal conductivity of uranium dioxide-silicon carbide composite fuel pellets prepared by Spark Plasma Sintering (SPS)." Journal of Nuclear Materials, 433 (1-3): 66-73.
- 10. J. E. Garay, S. C. Glade, U. Anselmi-Tamburini, P. Asoka-Kumar, Z. A. Munir, "Electric current enhanced defect mobility in Ni₃Ti intermetallics," Applied Physics Letters, 85 (2004) 573-575.
- 11. C. S. Bonifacio, T. B. Holland, K. van Benthem, "Evidence of surface cleaning during electric field assisted sintering," Scripta Materialia, 69 (2013) 769-772.
- 12. R. Baraki, S. Schwarz, O. Guillon, "Effect of electric field/current on sintering of fully stabilized zirconia," Journal of American Ceramic Society, 95 (2012) 75-78.
- 13. M. Cologna, A.L.G. Prette, R. Raj, "Flash sintering of cubic yttria-stabilized zirconia at 750C or possible use in SOFC manufacturing," Journal of American Ceramic Society, 94 (2011), 316-319.
- 14. J.G.P. Silva, J. Lebrun, H.A. Al-Qureshi, R. Janssen, R. Raj. "Temperature distributions during flash sintering of 8% yttria-stabilized zirconia," Journal of American Ceramic Society, 98 (2015), 3525-3528.
- 15. J.S.C. Francis, R. Raj, "Influence of the field and the current limit on flash sintering at isothermal furnace temperatures," Journal of American Ceramic Society, 96 (2013) 2754-2758.
- 16. E. Bichaud, J.M. Chaix, C. Carry, M. Kleitz, M.C. Steil. "Flash sintering incubation in Al₂O₃/TZP composites," Journal of European Ceramic Society, 35 (2015), 2587-2592.
- 17. Y. Dong, I.W. Chen, "Predicting the onset of flash sintering," Journal of American Ceramic Society, 98 (2015), 2333-2335.

- 18. R.I. Todd, E. Zapata-Solvas, R.S. Bonilla, T. Sneddon, P.R. Wilshaw, "Electrical characteristics of flash sintering: thermal runaway of joule heating," Journal of the European Ceramic Society, 35 (2015), 1865-1877.
- 19. Y. Dong, I.W. Chen, "Onset criterion for flash sintering," Journal of the American Ceramic Society, 98 (2015), 3624-3627.
- 20. J.G.P. Silva, H.A. Al-Qureshi, F. Keil, R. Janssen, "A dynamic bifurcation criterion for thermal runaway during flash sintering of ceramics," Journal of the European Ceramic Society, 36 (2016), 1261-1267.
- 21. Higgs, J.D., "Modelling Oxidation Behaviour In Operating Defective Nuclear Reactor Fuel Elements," Faculty of the Royal Military College of Canada, 2006.
- 22. K. Naito, T. Ishii, Y Hamaguchi, K. Oshima, X-ray study on phase transition of U₄O₉, Solid State Communications. **5** (1967) 349-352.